Polymer Journal
https://doi.org/10.1038/s41428-024-00908-7

FOCUS REVIEW

Design of functional soft interfaces with precise control of the polymer architecture

Tsukuru Masuda[1]

Received: 12 February 2024 / Revised: 3 March 2024 / Accepted: 4 March 2024

Abstract

Soft interfaces formed by polymer materials are important interfaces for biological systems (biointerfaces), and controlling their chemical and physical structures at the nanoscale plays an important role in understanding the mechanism and development of interface functionalities. Controlled radical polymerization (CRP) is highly suited for designing biointerfaces composed of polymer chains because it enables the formation of well-defined polymer brushes, block copolymers, and comb-type copolymers. This focus review describes the design of functional soft interfaces based on investigations of the structure-property relationships of CRPs. In particular, polymer brush surfaces showing autonomous property changes, 2D/3D transformations of lipid bilayers, and molecular interactions in bactericidal cationic polymer brushes are depicted.

Introduction

Soft interfaces are formed by polymers, colloids, and biomacromolecules and are nanometer-scale boundary regions composed of polymer chains, solvents, and ions. Among the various soft interfaces, synthetic polymers have attracted considerable attention because their structures and properties can be tuned artificially to achieve the desired functionalities [1–4]. One of their most important applications is as "biointerfaces," which are the interfaces between artificially designed materials (herein, polymeric interfaces) and biological systems (biomolecules and cells) (Fig. 1a). Biointerfaces formed by polymeric materials have been investigated for use in various applications, including biocompatible materials, cell culture materials, bioseparation systems, biomolecular recognition, drug delivery systems, and enzyme immobilization [5–13]. In these applications, the interactions between the artificial polymers and biological systems are important. Thermo and/or pH-responsive polymers that change their physicochemical properties dynamically in response to external stimuli have been extensively investigated for biomedical applications, in which structure control plays an important role, as summarized in reviews of polymer and interfacial science [14, 15]. As polymer materials with autonomous dynamic functions, "self-oscillating" polymers with built-in systems for energy conversion from chemical oscillation to mechanical oscillation have been developed and have become an area of great focus in advanced sciences [16]. As another important aspect of the interactions between biomolecules such as peptides and proteins and artificial polymers, accurate folding is essential for biological activities [17]. Overall, controlling the chemical and physical structures of interfaces at the nanoscale is important for investigating the mechanisms and development of functionalities.

In the field of polymer chemistry, controlled/living radical polymerizations (CRPs), such as atom transfer radical polymerization (ATRP) and reversible addition-fragmentation chain transfer (RAFT) polymerization, have been developed, enabling the preparation of well-controlled polymer architectures, including polymer brushes, block copolymers, and comb-type copolymers (Fig. 1b) [1, 18]. Importantly, the chain length, graft density, and chain-end functionalization can be systematically controlled to achieve the targeted functions. For example, high graft-density polymer brush surfaces can be prepared by surface-initiated ATRP (SI-ATRP), and zwitterionic polymer brush

✉ Tsukuru Masuda
masuda@bis.t.u-tokyo.ac.jp

[1] Department of Bioengineering, School of Engineering, The University of Tokyo, 7-3-1 Hongo, Bunkyo-ku, Tokyo 113-8656, Japan

Published online: 26 March 2024

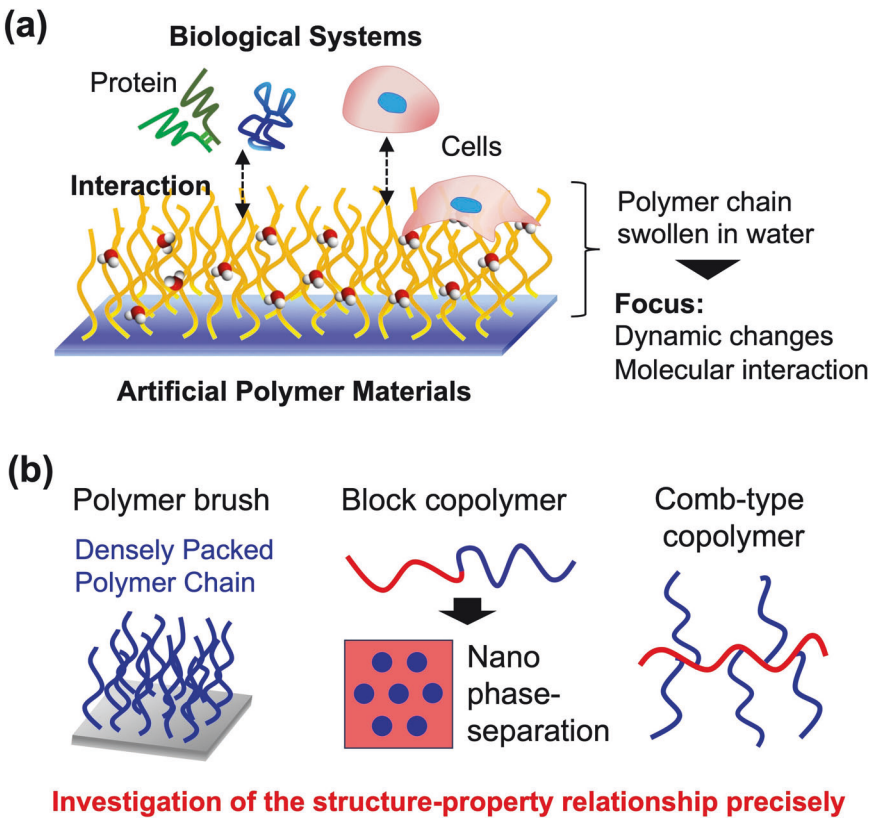

Fig. 1 Soft interfaces designed by controlled radical polymerization. **a** Illustration of soft interfacial contact with biological systems. **b** Structure-controlled polymers and soft interfaces prepared by controlled radical polymerization

surfaces have exhibited excellent fouling resistance [19]. Structural control of thermoresponsive polymer interfaces containing poly(*N*-isopropylacrylamide) (PNIPAAm), which dynamically changed their hydrophilic/hydrophobic properties, has been investigated for separation of biomolecules or cells [14, 15, 20]. More recently, CRP-based polymerization reactions that are highly suitable for biomaterials have also been developed. For example, activators regenerated by electron transfer (ARGET) ATRP proceed in aqueous media containing a reducing agent with tolerance to oxygen [21, 22]. Photoinduced electron transfer (PET) RAFT polymerization is also tolerant to oxygen and is suitable for high-throughput screening of polymers that interact with biomolecules or cells [23, 24]. Therefore, CRP techniques are very useful for designing biointerfaces.

This focus review presents functional soft interfaces showing autonomous motion and analyses of soft interfaces interacting with biological systems. The structure-property relationships were investigated by precise polymer architecture control. In particular, a polymer brush surface showing autonomous property changes coupled with an oscillating chemical reaction, 2D/3D transformations of lipid bilayers triggered by a comb-type copolymer, and interactions between proteins/bacteria and cationic polymer brushes to develop bactericidal surfaces are investigated.

Polymer brush surfaces with autonomous property changes and motion

Functional soft interfaces that dynamically change their physicochemical properties have attracted considerable attention and have been designed by grafting stimuli-responsive polymers [25–27]. If soft interfaces undergoing autonomous property changes without external stimuli are realized, they would contribute to novel applications such as autonomous mass transport systems at the micro- or nanoscale. Self-oscillating polymer brushes showing autonomous property changes, which involve energy conversion from an oscillating chemical reaction to the phase transitions of grafted polymer chains, have been developed (Fig. 2a) [28, 29]. The self-oscillating polymers were composed of NIPAAm and tris(2,2′-bipyridine)ruthenium [$Ru(bpy)_3$] as a catalyst for the Belousov–Zhabotinsky (BZ) reaction. They exhibited phase transitions at lower critical solution temperatures (LCSTs), and the LCST was shifted to a higher temperature when $Ru(bpy)_3$ was oxidized. Thus, the self-oscillating polymers exhibited periodic hydration/dehydration changes coupled with redox oscillations at a constant temperature [16, 30]. When the reaction medium (e.g., gels) is large, chemical wave propagation is generated as excited pulses of the oxidized state. To induce stable chemical wave propagation in the polymer brush, it was necessary to introduce dense and uniform polymer chains

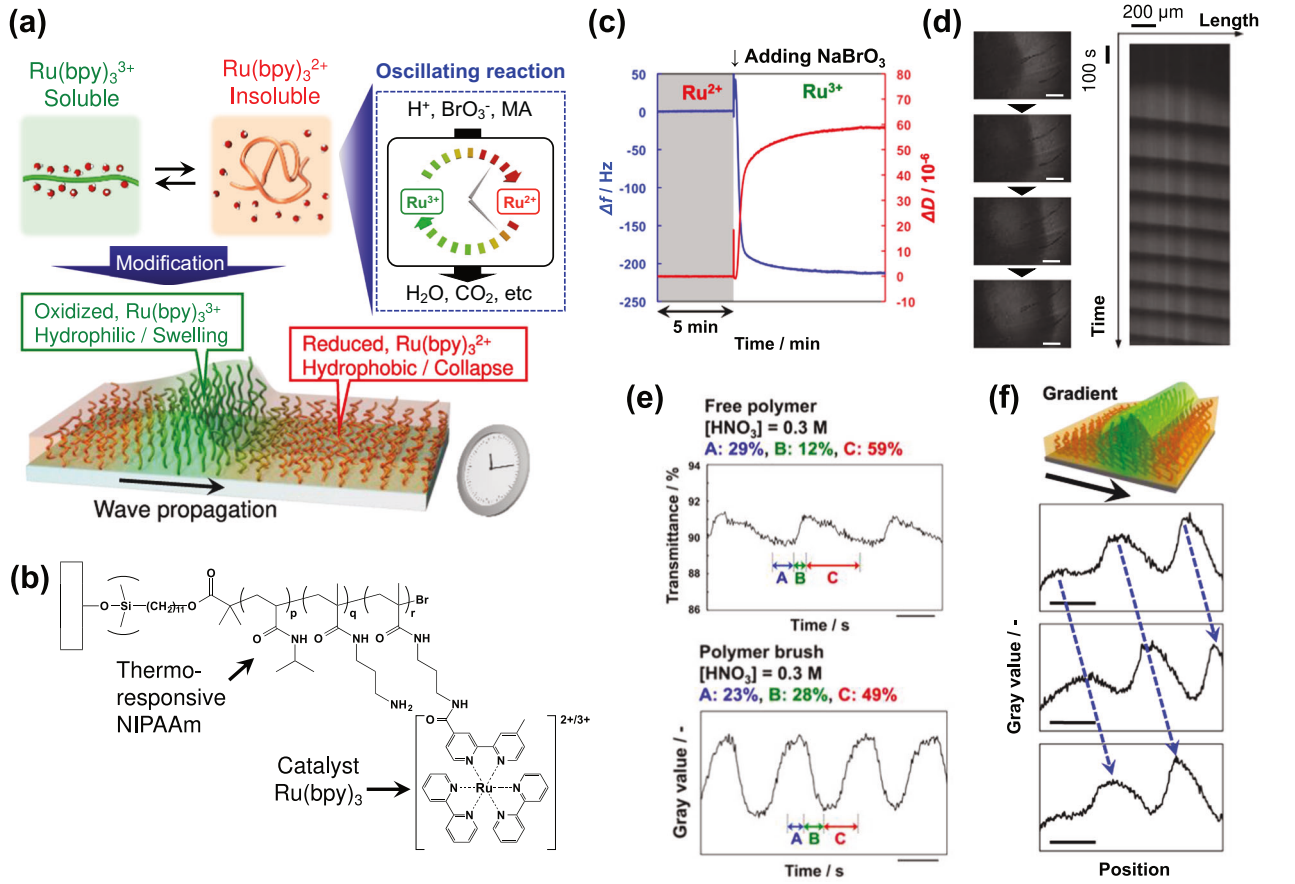

Fig. 2 Design of self-oscillating polymer brushes and their dynamic behaviors. **a** Illustration of the self-oscillating polymer brush showing autonomous property changes. **b** Chemical structure of poly(-NIPAAm-*co*-NAPMAm-*co*-Ru(bpy)$_3$NAPMAm). **c** Redox response of the polymer brush monitored by QCM-D. **d** Chemical wave propagation on the polymer brush. (a)-(d): Reproduced from ref. [29] with permission from the American Chemical Society. **e** Waveform analysis based on the FKN model. Scale: 50 s. Reproduced from ref. [33] with permission from the American Chemical Society. **f** Propagation direction control with a gradient structure. Scale: 500 μm. Reproduced under the terms of the Creative Commons CC BY license from ref. [34]

containing the Ru(bpy)$_3$ catalyst. Hence, SI-ATRP was used to prepare the target polymer brush surfaces. A polymer brush composed of NIPAAm and *N*-3-(aminopropyl) methacrylamide (NAPMAm) was prepared by SI-ATRP, followed by postmodification of Ru(bpy)$_3$ with *N*-hydroxysuccinimide ester on the amino groups of NAPMAm. In this manner, the substrate was modified with poly(-NIPAAm-*co*-NAPMAm-*co*-Ru(bpy)$_3$NAPMAm) brush as a self-oscillating polymer brush (Fig. 2b). The structure of the polymer-grafted surface was characterized by X-ray photoelectron spectroscopy, attenuated total reflectance Fourier transform infrared spectroscopy (ATR/FT-IR), and UV–vis spectroscopy. Swelling of the grafted polymer chains was analyzed using a quartz crystal microbalance with dissipation (QCM-D). The lower frequency and increased energy dissipation after the addition of an oxidizing agent indicated that the polymer brush was swollen due to oxidation of the Ru(bpy)$_3$ moiety (Fig. 2c). To investigate the oscillations of the polymer brushes, the polymer brush-grafted glass substrates were immersed in an aqueous solution containing HNO_3, $NaBrO_3$ and malonic acid and studied with fluorescence microscopy. Stable chemical wave propagation was achieved by appropriately designing the polymer brush surface (Fig. 2d). The grafted amounts of polymer and immobilized Ru(bpy)$_3$ on the polymer brush, as shown in Fig. 2d, were 7.7 μg cm^{-2} and 1.7 nmol cm^{-2}, respectively. Inadequate or excessive amounts of Ru(bpy)$_3$ resulted in no oscillations or shorter oscillation durations. These evaluations provide guidelines for suitable design of polymer brush surfaces undergoing autonomous property changes [29]. Self-oscillation of the polymer brush was also detected as a periodic electrical response in a solution-gated ion-sensitive field-effect transistor (ISFET) [31].

In self-oscillating polymer brushes, the polymer chains with the catalyst are densely packed on the solid substrate; thus, the self-oscillating behavior is likely to be affected by dense localization of the catalyst, as the diffusion of intermediates in the BZ reaction tunes the rhythms or patterns. To clarify this, the waveform of the self-oscillating polymer brush was analyzed with the Field–Körös–Noyes (FKN)

model [32] by comparing the waveform with those of the free polymer and gel. According to the FKN model, the BZ reaction was divided into the following three processes: process A, consumption of the inhibitor (bromide ion, Br); process B, autocatalytic reaction of bromous acid ($HBrO_2$) with oxidation of the catalyst; and process C, an organic reaction with reduction of the catalyst. Generally, process B is rapid because it is an autocatalytic reaction. For the self-oscillating polymer brush, the rate of process B was lower than that of the free polymer brush (Fig. 2e). This was attributed to immobilization of the catalyst onto the densely packed polymer chain, reducing accessibility of the reacting substrates to the catalyst (immobilization effect) [33].

Considering the potential application of self-oscillating polymer brushes in mass transport systems, direction control of the chemical waves is an important issue. To this end, a self-oscillating polymer brush with gradient thickness was prepared using sacrificial anode ATRP. The thickness was in the range of several tens of nanometers, and the amount of $Ru(bpy)_3$ increased as the thickness (or grafted amount) increased. The gradient polymer brush induced unidirectional chemical wave propagation from a region with small amounts of $Ru(bpy)_3$ to that with large amounts of $Ru(bpy)_3$ [34]. Furthermore, control of the propagating chemical waves in the self-oscillating polymer brush was achieved by introducing a pentagonal-patterned structure [35]. In summary, polymer brush surfaces with autonomous property changes were designed (self-oscillating polymer brushes). The polymer brush surfaces exhibited unique properties: (1) autonomous property changes were induced with constant external conditions, and (2) locally induced property changes propagated coupled with diffusion. These functions at the nanoscale interface were designed by the CRP and self-organization of an out-of-equilibrium living system.

In addition, the design of poly(NIPAAm-*co*-NAPMAm-*co*-$Ru(bpy)_3$NAPMAm), a self-oscillating polymer prepared by a postmodification method, contributed to chemo-mechanical oscillation of the gels. For the use of self-oscillating gels as autonomous actuators, an increase in volume, an increase in the working temperature range, and oscillations of the mold solution conditions are needed. By controlling the conjugation ratio of $Ru(bpy)_3$ in the ternary copolymer, volume oscillation was achieved near physiological temperatures (37 °C) [36]. Furthermore, autonomous swelling-deswelling oscillation of a gel composed of poly(NIPAAm-*co*-NAPMAm-*co*-$Ru(bpy)_3$NAPMAm) was achieved in a hydrated protic ionic liquid (PIL) serving as a proton source for the BZ reaction, which contributed to the development of self-oscillating gels under mild conditions [37]. Thus, the chemical structure of a polymer plays an important role in controlling its self-oscillating behavior. A self-oscillating polymer containing a ureido group that exhibited an upper critical solution temperature (UCST)-type phase transition has also been reported [38].

Polymer-driven 2D/3D transformations of lipid bilayers

Lipid bilayer transformations occur in various biological phenomena. Hence, the design of artificial materials to manipulate lipid membrane dynamics could provide novel information and tools for bioscience and biotechnology, thereby enabling access to the membranes of cells or liposomes. Generally, transformations from 3D lipid vesicles to 2D nanosheets are thermodynamically prohibited because the apolar/polar interfaces between the hydrophobic bilayer edges and water are energetically unfavorable. To date, only mesoscopic lipid sheet formation by ERM family proteins or synthetic amphiphiles has been reported [39, 40], whereas quantitative regulation of lipid sheet formation under physiological conditions remains challenging.

In an attempt to control the structures and functions of peptides with ionic graft copolymers, cell-sized 3D lipid vesicles were quantitatively transformed into mesoscopic 2D lipid bilayer nanosheets by adding an amphiphilic E5 peptide and a cationic comb-type copolymer (Fig. 3a) [41]. The E5 peptide is an anionic, amphiphilic, membrane-disruptive peptide that mimics the N-terminal region of hemagglutinin [42]. A cationic comb-type copolymer composed of a cationic backbone and dense grafts of hydrophilic dextran (poly(allylamine)-*graft*-dextran (PAA-*g*-Dex); Dex: 92 wt%) had a chaperone-like function in anionic E5; that is, it induced E5 to form a membrane-active helix structure [43]. During lipid nanosheet formation, the E5/PAA-*g*-Dex complex was expected to stabilize the lipid/water nanometer-order interfaces at the edges of the lipid nanosheets. Since the hydrophilic grafts of the copolymer could decrease the apolar/polar interfacial energy, the density of the hydrophilic grafts was hypothesized to be a key factor in nanosheet formation. Hence, to reveal the mechanisms underlying the formation of lipid nanosheets, the structural effects of cationic copolymers on nanosheet formation were systematically investigated.

Cationic comb-type copolymers were prepared by reductive amination using various ratios of Dex (M_w: 1.1×10^4) or poly(ethylene glycol) (PEG) (M_w: 4.8×10^3) (Fig. 3b). The Dex and PEG contents varied from 6 to 26 mol% and from 6 to 19 mol%, respectively. The structures of E5 with and without the copolymers were investigated using circular dichroism (CD). PAA-*g*-Dex induced folding of the E5 peptide into a helical structure, whereas E5 alone formed a random coil at pH 7.4 (Fig. 3c). PAA-*g*-PEG also induced the folding of E5. When the Dex content

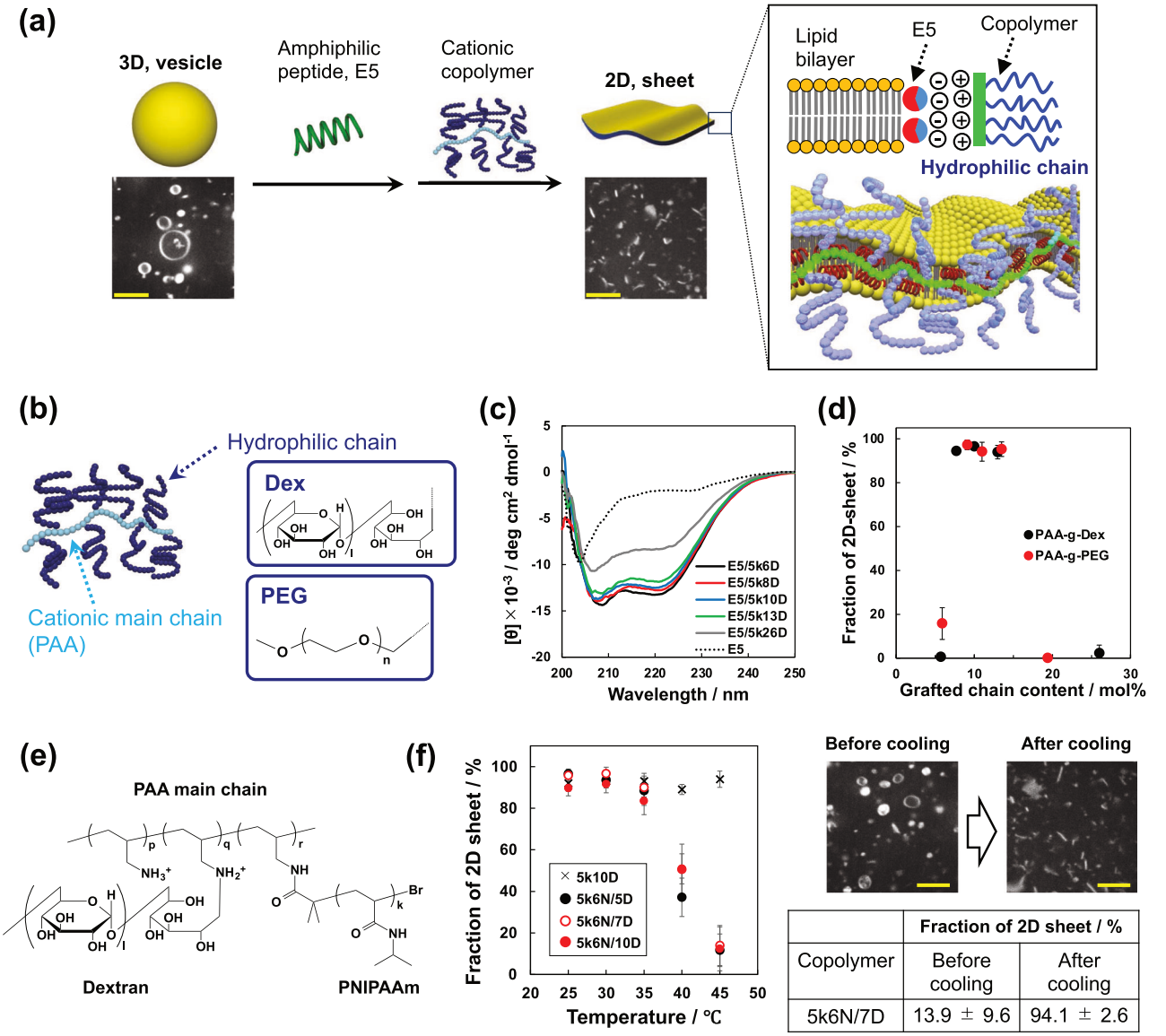

Copolymer	Fraction of 2D sheet / %	
	Before cooling	After cooling
5k6N/7D	13.9 ± 9.6	94.1 ± 2.6

Fig. 3 2D/3D transformation of lipid bilayers controlled by the peptide and comb-type copolymer. **a** The amphiphilic E5 peptide and the cationic comb-type copolymer induced 2D lipid nanosheet formation. Scale: 10 μm. **b** Structures of the cationic comb-type copolymers. **c** CD spectra of the E5 peptide with/without the copolymers. **d** Fraction of 2D sheets as a function of the grafted chain content. **e** Structure of the hetero-grafted copolymer. **f** Left: Temperature dependency of the 2D sheet fraction with the hetero-grafted copolymer. Right: 2D sheet formation triggered by temperature changes. The samples are referred to as 5k*X*N/*Y*D, where N indicates the NIPAAm and *X* and *Y* are the mol% of the grafted PNIPAAm and Dex, respectively. Reproduced from ref. [45] with permission from the American Chemical Society

was 26 mol%, the helical content was lower than those of the other copolymers, which was attributed to the steric hindrance caused by the dextran-grafted chain. To investigate the lipid bilayer transformation, E5 and the copolymer were added to a giant vesicle composed of 1,2-dioleoyl-*sn*-glycero-3-phosphatidylcholine (DOPC), and the samples were observed with fluorescence confocal microscopy. When the concentrations of E5 and the copolymers were 10 μM and 6.9 μM, respectively, almost all lipid membranes were transformed into nanosheets by copolymers with a certain range of hydrophilic grafted chain contents. Figure 3d summarizes the fractions of lipid nanosheets formed in the presence of E5 (10 μM) and the cationic copolymers (6.9 μM) as a function of the content of the hydrophilic grafted chains. Notably, lipid nanosheet formation was controlled in an all-or-nothing manner when the graft content of the copolymer was increased from 5.7 mol % to 7.7 mol % for both PAA-*g*-Dex and PAA-*g*-PEG. For copolymers with low hydrophilic chain contents, a decrease in the hydrophobic/hydrophilic interfacial energy would not be sufficient to stabilize the nanosheets. For the upper limit of the grafted-chain content, the densely grafted chains likely inhibited the interaction with E5 compared with the other copolymers.

This finding prompted us to develop a polymer-driven smart 2D/3D transformation system for lipid bilayers, given that slight changes in the properties of the grafted chains would cause 2D/3D transformations. Hetero-grafted copolymers with thermoresponsive PNIPAAm and dextran-grafted chains were designed (Fig. 3e). In a previous study, a cationic comb-type copolymer comprising thermoresponsive PNIPAAm as the grafted chain (PAA-*g*-PNIAAm) was synthesized, and its interactions with the anionic E5 peptide were investigated [44]. PAA-*g*-PNIPAAm also induced the formation of the helical structure of E5, whereas the copolymer formed micelle-like aggregates above the LCST. As aggregation is undesirable in the function of E5 [43], a hetero-grafted PAA-*g*-Dex/PNIPAAm was designed (Fig. 3e). PAA-*g*-PNIPAAm was synthesized by a "grafting from" method using activators regenerated by electron-transfer atom-transfer radical polymerization (ARGET ATRP), followed by conjugation of Dex to obtain the target hetero-grafted copolymer. The number-averaged hydrodynamic diameters (D_h) of the copolymers were measured as a function of temperature using dynamic light scattering (DLS). The D_h value exceeded the transition temperature, which decreased as the dextran content in the hetero-grafted copolymer increased. Furthermore, fluorescence measurements using pyrene as a hydrophobic probe indicated that the PNIPAAm grafts exhibited thermoresponsive coil–globule transitions without inhibition by the dextran grafts. CD spectra indicated that the hetero-grafted copolymers induced helical structure formation in E5 both below and above the LCST. Finally, the effect of the thermoresponsiveness of the hetero-grafted copolymers on the lipid bilayer transformation was evaluated. For the hetero-grafted copolymers, the nanosheet fraction decreased at temperatures above 35 °C, decreasing to below 15% at 45 °C. The PNIPAAm grafts became hydrophobic and collapsed above the LCST, thereby failing to stabilize the edges of the lipid nanosheets above 35 °C. Moreover, 2D/3D transformations of cell-sized lipid bilayers were triggered by temperature changes (Fig. 3f) [45]. The soft materials that dynamically transformed the lipid membranes could contribute to life sciences and engineering because liposomes are widely utilized in medicines, foods, and cosmetics.

Analyses of the molecular interactions between well-controlled cationic polymer brushes and biological systems

Polyelectrolyte brushes have attracted considerable attention as functional soft interfaces. Among these, cationic polyelectrolyte brushes containing quaternary ammonium (QA) moieties are particularly attractive because of their potential to provide bactericidal surfaces [46, 47]. In a previous study, the killing efficacy increased with increasing graft density, which was controlled by increasing the initiator concentration from 0.01 to 100% [47]. The conformational changes with graft density were estimated in this initiator concentration range, as the mushroom-to-brush crossover was observed at approximately 0.1 chains nm^{-2} [48]. Hence, the graft density was a key parameter determining the bactericidal properties. However, the relationship between the grafted structure and the adsorbed state of bacteria has not been studied. Therefore, a well-controlled polymer brush structure with a QA moiety is required to explain the underlying bactericidal mechanism in detail.

In this study, cationic poly(2-(methacryloyloxy)ethyl) trimethylammonium chloride) (PMTAC) brush surfaces were systematically prepared using SI-ATRP (Fig. 4a), and the factors affecting their bactericidal properties and interactions with proteins are discussed. The graft density was successfully controlled with the [11-(2-bromo-2-methyl) propionyloxy] undecyltrichlorosilane (BrC11TCS; an ATRP initiator) ratio of BrC11TCS/(BrC11TCS + dodecyltrichlorosilane) in the silane coupling reaction. Specifically, high-graft-density (0.45 chains nm^{-2}; sufficiently higher than 0.1 chains nm^{-2}) and low-graft-density (0.06 chains nm^{-2}) surfaces were prepared. The obtained PMTAC brush surfaces were hydrophilic, as indicated by contact angle measurements. The zeta potential dependence of the PMTAC brushes was analyzed with Smolchowski's equation and the Gouy–Chapman model, which described the diffusive electric double layer. This measurement indicated that the PMTAC brushes were positively charged; thus, the molecular interactions on the surface could be examined on the basis of electrostatic interactions. The amount of protein adsorbed on the polymer brush surfaces in a phosphate-buffered saline (PBS) solution (pH 7.4) was quantified using QCM-D. The frequency shift corresponded to the amount of adsorbed protein. Here, BSA (isoelectric point, pI: 4,7) and lysozyme (pI: 11.4) were used as negatively and positively charged proteins, respectively. For the high-graft-density brushes, the frequency shifts for BSA and lysozyme adsorption were large and small, respectively (Fig. 4b). This indicated that protein adsorption by the high-graft-density cationic polymer brushes was regulated by electrostatic interactions. As the graft density decreased, lysozyme adsorption increased. This was attributed to adsorption on the surface and adsorption in the spaces within the low-density grafted polymer chains [49]. Subsequently, the bactericidal activities of the polymer brushes were evaluated. Figure 4c shows fluorescence microscopy images of a live/dead assay of *Staphylococcus aureus* (*S. aureus*) adhered to PMTAC brush surfaces in nutrient-rich trypticase soy broth (TSB). The zeta potential of *S. aureus* was reported to be −37.1 mV [50], and bacterial adhesion was thought to be promoted by electrostatic interactions

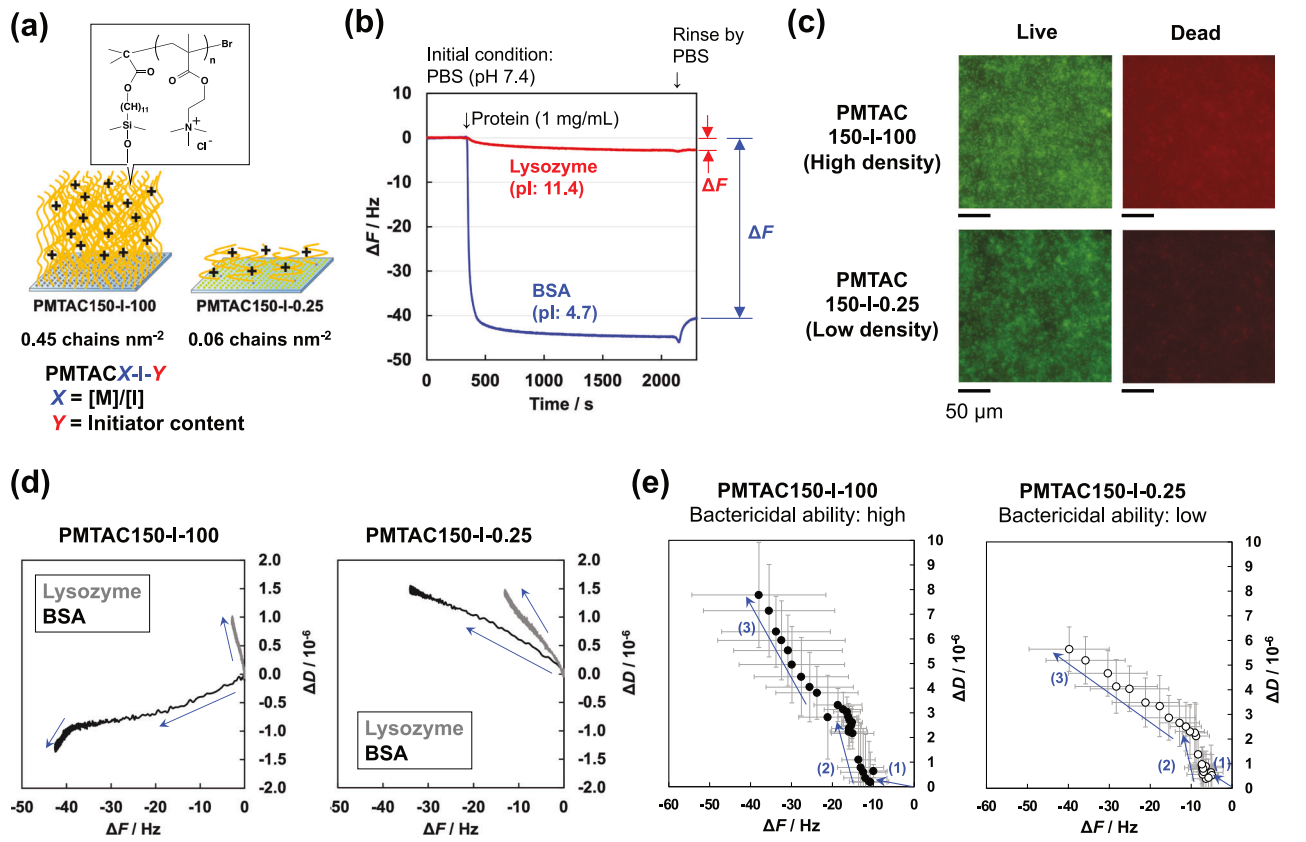

Fig. 4 Analysis of the interactions at the biointerface of the well-controlled cationic polymer brush. **a** Illustration of the PMTAC polymer brushes. **b** QCM chart for protein adsorption onto the high-graft-density PMTAC polymer brush. **c** Live/dead assay for *S. aureus* on PMTAC polymer brushes. **d** ΔD–ΔF plot for protein adsorption onto the PMTAC polymer brushes. **e** ΔD–ΔF plots for *S. aureus* adhering to PMTAC polymer brushes. Reproduced from ref. [52] with permission from the American Chemical Society

with the negatively charged bacterial surface. The signal indicating dead cells on the high-graft-density surface (0.45 chains nm^{-2}) was significantly greater than that on the low-graft-density surface (0.06 chains nm^{-2}). Because contact between the polymer brush and the bacterial membrane was required to kill bacteria, the high efficiency of the high-graft-density PMTAC brush surface was attributed to the increased contact area between the polymer brush surface and the bacterium.

To determine the mechanism for the bactericidal properties of the high-graft-density PMTAC brush surfaces, the adsorption state analyzed with the energy dissipation factor monitored by QCM-D (Fig. 4d). For lysozyme adsorption, the ΔD was positive for both polymer brush surfaces, which is typical for protein adsorption. For BSA adsorption, the ΔD on the high-graft-density surface was negative, while that on the low-graft-density surface was positive. These results indicated that the adsorption of negatively charged BSA on the cationic polymer brush was dependent on the graft density. In particular, the negative ΔD shifts indicated that the BSA-adsorbed, high-graft-density PMTAC brush became rigid. Similar behavior was observed when adsorption of the solutes in the TSB medium was analyzed. Negative ΔD values in protein adsorption analyses by QCM-D are not typically observed. Previous studies reported similar phenomena, for example, with adsorption of a C-reactive protein onto a zwitterionic phosphorylcholine-immobilized surface [51]. Negative ΔD shifts indicate strong interactions between proteins and material surfaces and water release from the proteins and/or material surfaces. Furthermore, adhesion of *S. aureus* to the PMTAC brush surfaces under culture conditions was analyzed using QCM-D (Fig. 4e). The small slopes of the $\Delta D/\Delta F$ plots showed that the initially adsorbed bacteria interacted strongly with the high-graft-density polymer brush compared to the low-graft-density polymer brush (slope (1) in Fig. 4e). The slope (3) of the high-graft-density surface was relatively large. This suggested that the killed bacteria were not adhered firmly, which was attributed to the bactericidal activity. These precise analyses of molecular interactions in well-controlled cationic polymer brushes will contribute to the design of antibacterial surfaces [52]. In designing antibacterial surfaces, removal of the bacteria from the material surface is an important issue, and biointerfaces showing simultaneous bactericidal and antibiofouling properties have attracted great attention [53, 54]. Bacterial repellent interfaces can be prepared by surface modifications

of zwitterionic polymers, and bacterial adhesiveness is dependent on the structure of the cross-linked phospholipid copolymer surface [55]. Based on these studies, precise structure–property relationships and interaction analyses will play important roles in enhancing antibacterial properties.

In designing biointerfaces, protein–material interactions are key fundamental processes, and a well-controlled model interface is useful for understanding the factors involved in these interactions. As described above, protein adsorption on high-graft-density PMTAC surfaces was regulated by electrostatic interactions (Fig. 4b). The high-graft-density polymer brush surface is a suitable interface for analyzing adsorption by removing factors induced by the physical structure, such as protein adsorption inside polymer chains. In a previous study, the effects of chemical factors and water structure on protein adsorption were investigated by synthesizing various types of surfaces (hydrophobic, hydrophilic, anionic, cationic, and zwitterionic) with polymer brushes [56]. The use of block copolymers is a suitable method for investigating the physical structural factors because they can form nanophase-separated structures. By designing phase-separated surfaces with different hydrophobic domain sizes (10 or 20 nm) based on amphiphilic ABA-type block copolymers, a protein smaller than the nanoscale hydrophobic domains (herein lysozyme) was adsorbed on the phase-separated surface [57]. Thus, structure-controlled model surfaces are useful for understanding the factors related to protein adsorption, which are typically complicated and difficult to predict.

Conclusion and future perspective

This review described functional soft interfaces achieved by precise control of polymer architecture with CRP. Investigations of the structure-property relationships are important for designing biomimetic dynamic soft interfaces, which reveal the mechanisms for the molecular interactions and resulting biological activities; in particular, polymer brush surfaces showed autonomous property changes, comb-type copolymer-mediated 2D/3D transformations of lipid bilayers, and molecular interactions of bactericidal cationic polymer brushes. Importantly, precise control of the polymer interfacial structure enabled the desired functions in these systems, even though the molecular interactions and dynamic processes are complex.

Since the interactions at soft/biointerfaces are complicated by various chemical and physical factors, the design of biointerfaces that show targeted functions in a predictable manner remains challenging. Another important factor is that biological systems are out of equilibrium during continuous chemical reactions; thus, the conditions of biomolecules are affected by these chemical reactions. For example, in enzymatic reactions, accelerated diffusion of an enzyme due to released heat has been reported (chemoacoustic effect) [58]. To consider such complicated interactions between biological systems and artificial polymers, structure–property relationships developed with theory and modeling are needed. Recently, machine learning has been applied to biointerface design to predict interfacial properties such as protein adsorption [59, 60]. Hence, new theories and technologies can advance our understanding of the mechanisms and soft interfaces that are adaptable to biologically active systems.

Acknowledgements The author would like to express gratitude to Professor Madoka Takai (The University of Tokyo) for supervision and support. The authors are grateful to Professors Atsushi Maruyama (Tokyo Institute of Technology), Ryo Yoshida (The University of Tokyo), Teruo Okano (University of Utah), Aya M. Akimoto (Ochanomizu University), Naohiko Shimada (Tokyo Institute of Technology), and Kenichi Nagase (Keio University) for their support and encouragement. The authors thank the Japan Society for the Promotion of Science (JSPS) for providing support through a Grant-in-Aid for Scientific Research (B) (No. 20H02795 to T.M.). We thank AJE for editing the English grammar.

Funding Open Access funding provided by The University of Tokyo.

Compliance with ethical standards

Conflict of interest The authors declare no competing interests.

Publisher's note Springer Nature remains neutral with regard to jurisdictional claims in published maps and institutional affiliations.

References

1. Pester CW, Klok H-A, Benetti EM. Opportunities, challenges, and pitfalls in making, characterizing, and understanding polymer brushes. Macromolecules. 2023;56:9915–38.
2. Wang R, Wei Q, Sheng W, Yu B, Zhou F, Li B. Driving polymer brushes from synthesis to functioning. Angew Chem Int Ed. 2023;62:e202219312.
3. Yokoyama H. New developments in polymer brush fabrication: concepts and physical properties of dynamic polymer brushes. Polym J. 2023;55:735–42.
4. Masuda T, Takai M. Design of biointerfaces composed of soft materials using controlled radical polymerizations. J Mater Chem B. 2022;10:1473–85.

5. Lin X, Wu K, Zhou Q, Jain P, Boit MO, Li N, et al. Photoreactive carboxybetaine copolymers impart biocompatibility and inhibit plasticizer leaching on polyvinyl chloride. ACS Appl Mater Interfaces. 2020;12:41026–37.
6. Okihara M, Matsuda A, Kawamura A, Miyata T. Design of dual stimuli-responsive gels with physical and chemical properties that vary in response to light and temperature and cell behavior on their surfaces. Polym J. 2024;56:193–204.
7. Ogiwara N, Nakano T, Masuda T, Kushiro K, Takai M. Cell spheroid formation on the surface of multi-block copolymers composed of Poly (2-methoxyethyl acrylate) and polyethylene glycol. Macromol Biosci. 2023;23:2200486.
8. del Castillo GF-D, Kyriakidou M, Adali Z, Xiong K, Hailes RLN, Dahlin A. Electrically switchable polymer brushes for protein capture and release in biological environments. Angew Chem Int Ed 2022;61:e202115745.
9. Nagase K, Nishiyama T, Inoue M, Kanazawa H. Temperature responsive chromatography for therapeutic drug monitoring with an aqueous mobile phase. Sci Rep. 2021;11:23508.
10. Wu J-G, Wei S-C, Luo S-C. In situ probing unusual protein adsorption behavior on electrified zwitterionic conducting polymers. Adv Mater Interfaces. 2020;7:2000470.
11. Nagao M, Masuda T, Takai M, Miura Y. Preparation of cellular membrane-mimicking glycopolymer interfaces by the solvent-assisted method on QCM-D sensor chips and their molecular recognition. J Mater Chem B. 2024;12:1782–7.
12. Fujii S. Polymeric core-crosslinked particles prepared via a nanoemulsion-mediated process: from particle design and structural characterization to in vivo behavior in chemotherapy. Polym J. 2023;55:921–33.
13. Sánchez-Morán H, Gonçalves LRB, Schwartz DK, Kaar JL. Framework for optimizing polymeric supports for immobilized biocatalysts by computational analysis of enzyme surface hydrophobicity. ACS Catal. 2023;13:4304–15.
14. Hiruta Y. Poly(*N*-isopropylacrylamide)-based temperature- and pH-responsive polymer materials for application in biomedical fields. Polym J. 2022;54:1419–30.
15. Nagase K. Thermoresponsive interfaces obtained using poly(*N*-isopropylacrylamide)-based copolymer for bioseparation and tissue engineering applications. Adv Colloid Interface Sci. 2021;295:102487.
16. Yoshida R. Creation of softmaterials based on self-oscillating polymer gels. Polym J. 2022;54:827–49.
17. Hanpanich O, Maruyama A. Cationic comb-type copolymer as an artificial chaperone. Polym J. 2019;51:935–43.
18. Corrigan N, Jung K, Mood G, Hawker CJ, Matyjaszwewski K, Boyer C. Reversible-deactivation radical polymerization (Controlled/living radical polymerization): From discovery to materials design and applications. Prog Polym Sci. 2020;111:101311.
19. Higaki Y, Kobayashi M, Murakami D, Takahara A. Anti-fouling behavior of polymer brush immobilized surfaces. Polym J. 2016;48:325–31.
20. Nagase K, Kojima N, Goto M, Akaike T, Kanazawa H. Thermoresponsive block copolymer brush for temperature-modulated hepatocyte separation. J Mater Chem B. 2022;10:8629–41.
21. Hong D, Hung H-C, Wu K, Lin X, Sun F, Zhang P, et al. Achieving ultralow fouling under ambient conditions via surface-initiated ARGET ATRP of carboxybetaine. ACS Appl Mater Interfaces. 2017;9:9255–9.
22. Szczepaniak G, Fu L, Jafari H, Kapil K, Matyjaszewski K. Making ATRP More Practical: Oxygen Tolerance. Acc Chem Res. 2021;54:1779–90.
23. Ng G, Li M, Yeow J, Jung K, Pester CW, Boyer C. Benchtop Preparation of Polymer Brushes by SI-PET-RAFT: The Effect of the Polymer Composition and Structure on Inhibition of a Pseudomonas Biofilm. ACS Appl Mater Interfaces. 2020;12:55243–54.
24. Tamasi MJ, Patel RA, Borca CH, Kosuri S, Mugnier H, Upadhya R, et al. Machine learning on a robotic platform for the design of polymer–protein hybrids. Adv Mater. 2022;34:2201809.
25. Li D, Xu L, Wang J, Gautrot JE. Responsive polymer brush design and emerging applications for nanotheranostics. Adv Healthc Mater 2021;10:2000953.
26. Matsukawa K, Masuda T, Kim YS, Akimoto AM, Yoshida R. Thermoresponsive surface-grafted gels: controlling the bulk volume change properties by surface-localized polymer grafting with various densities. Langmuir. 2017;33:13828–33.
27. Dunderdale GJ, Fairclough JPA. Coupling pH-responsive polymer brushes to electricity: switching thickness and creating waves of swelling or collapse. Langmuir. 2013;29:3628–35.
28. Masuda T, Hidaka M, Murase Y, Akimoto AM, Nagase K, Okano T, et al. Self-oscillating polymer brushes. Angew Chem Int Ed. 2013;52:7468–71.
29. Masuda T, Akimoto AM, Nagase K, Okano T, Yoshida R. Design of self-oscillating polymer brushes and control of the dynamic behaviors. Chem Mater. 2015;27:7395–402.
30. Yoshida R, Takahashi T, Yamaguchi T, Ichijo H. Self-Oscillating Gel. J Am Chem Soc. 1996;118:5134–5.
31. Sakata T, Nishitani S, Yasuoka Y, Himori S, Homma K, Masuda T, et al. Self-oscillating chemoelectrical interface of solution-gated ion-sensitive field-effect transistor based on Belousov–Zhabotinsky reaction. Sci Rep. 2022;12:2949.
32. Field RJ, Körös E, Noyes RM. Oscillations in chemical systems. II. Through analysis of temporal oscillation in the bromate-cerium-malonic acid system. J Am Chem Soc. 1972;94:8649–64.
33. Masuda T, Akimoto AM, Furusawa M, Tamate R, Nagase K, Okano T, et al. Aspects of the Belousov−Zhabotinsky reaction inside a self-oscillating polymer brush. Langmuir. 2018;34:1673–80.
34. Masuda T, Akimoto AM, Nagase K, Okano T, Yoshida R. Artificial cilia as autonomous nanoactuators: Design of a gradient self-oscillating polymer brush with controlled unidirectional motion. Sci Adv. 2016;2:e1600902.
35. Homma K, Masuda T, Akimoto AM, Nagase K, Itoga K, Okano T, et al. Fabrication of micropatterned self-oscillating polymer brush for direction control of chemical waves. Small. 2017;13:1700041.
36. Masuda T, Terasaki A, Akimoto AM, Nagase K, Okano T, Yoshida R. Control of swelling-deswelling behavior of a self-oscillating gel by designing the chemical structure. RSC Adv. 2015;5:5781.
37. Masuda T, Ueki T, Tamate R, Matsukawa K, Yoshida R. Chemomechanical motion of a self-oscillating gel in a protic ionic liquid. Angew Chem Int Ed. 2018;57:16693–7.
38. Masuda T, Shimada N, Sasaki T, Maruyama A, Akimoto AM, Yoshida R. Design of a tunable self-oscillating polymer with ureido and $Ru(bpy)_3$ moieties. Angew Chem Int Ed. 2017;56:9459.
39. Saitoh A, Takiguchi K, Tanaka Y, Hotani H. Opening-up of liposomal membranes by talin. Proc Natl Acad Sci. 1998;95:1026–31.
40. Hamada T, Sugimoto R, Vestergaard MC, Nagasaki T, Takagi M. Membrane disk and sphere: controllable mesoscopic structures for the capture and release of a targeted object. J Am Chem Soc. 2010;132:10528–32.
41. Shimada N, Kinoshita H, Umegae T, Azumai S, Kume N, Ochiai T, et al. Cationic Copolymer-Chaperoned 2D-3D Reversible Conversion of Lipid Membranes. Adv Mater. 2019;31:1904032.
42. Murata M, Kagiwada S, Takahashi S, Ohnishi S. Membrane fusion induced by mutual interaction of the two charge-reversed amphiphilic peptides at natural pH. J Biol Chem. 1991;266:14353–8.
43. Shimada N, Kinoshita H, Tokunaga S, Umegae T, Kume N, Sakamoto W, et al. Inter-polyelectrolyte nano- assembly induces folding and activation of functional peptides. J Controlled Release. 2015;281:45–52.

44. Masuda T, Shimada N, Maruyama A. A thermoresponsive cationic comb-type copolymer enhances membrane disruption activity of an amphiphilic peptide. Biomacromolecules. 2018;19:1333–9.
45. Masuda T, Takahashi S, Ochiai T, Yamada T, Shimada N, Maruyama A. Autonomous Vesicle/Sheet Transformation of Cell-Sized Lipid Bilayers by Hetero-Grafted Copolymers. ACS Appl Mater Interfaces. 2022;14:53558–66.
46. Ye G, Lee J, Perreault F, Elimelech M. Controlled architecture of dual-functional block copolymer brushes on thin- film composite membranes for integrated "defending" and "attacking" strategies against biofouling. ACS Appl Mater Interfaces. 2015;7:23069–79.
47. Murata H, Koepsel R, Matyjaszewski K, Russell AJ. Permanent, non-leaching antibacterial surfaces 2: How high density cationic surfaces kill bacterial cells. Biomaterials. 2007;28:4870–9.
48. Wu T, Efimenko K, Genzer J. Combinatorial study of the mushroom-to-brush crossover in surface anchored polyacrylamide. J Am Chem Soc. 2002;124:9394–5.
49. Feng W, Brash JL, Zhu S. Non-biofouling materials prepared by atom transfer radical polymerization grafting of 2- methacryloloxyethyl phosphorylcholine: Separate effects of graft density and chain length on protein repulsion. Biomaterials. 2006;27:847–55.
50. Oh J-K, Yegin Y, Yang F, Zhang M, Li J, Huang S, et al. The influence of surface chemistry on the kinetics and thermodynamics of bacterial adhesion. Sci Rep. 2018;8:17247.
51. Wu J-G, Wei S-C, Chen Y, Chen J-H, Luo S-C. Critical study of the recognition between C-reactive protein and surface- immobilized phosphorylcholine by quartz crystal microbalance with dissipation. Langmuir. 2018;34:943–51.
52. Masuda T, Watanabe Y, Kozuka Y, Saegusa Y, Takai M. Bactericidal ability of well-controlled cationic polymer brush surfaces and the interaction analysis by quartz crystal microbalance with dissipation. Langmuir. 2023;39:16522–31.
53. Ko Y, Truong VK, Woo SY, Dickey MD, Hsiao L, Genzer J. Counterpropagating gradients of antibacterial and antifouling polymer brushes. Biomacromolecules. 2022;23:424–30.
54. Ye G, Lee J, Perreault F, Elimelech M. Controlled architecture of dual-functional block copolymer brushes on thin-film composite membranes for integrated "defending" and "attacking" strategies against biofouling. ACS Appl Mater Interfaces. 2015;7:23069–79.
55. Lu Z, Mondarte EAQ, Suthiwanich K, Hayashi T, Masuda T, Isu N, et al. Study on bacterial antiadhesiveness of stiffness and thickness tunable cross-linked phospholipid copolymer thin-film. ACS Appl Bio Mater. 2020;3:1079–87.
56. Nagasawa D, Azuma T, Noguchi H, Uosaki K, Takai M. Role of interfacial water in protein adsorption onto polymer brushes as studied by SFG spectroscopy and QCM. J Phys Chem C. 2015;119:17193–201.
57. Masuda T, Hitaguchi Y, Kushiro K, Araki Y, Wada T, Takai M. Protein adsorption behavior in nanoscale phase-separated polymer coatings T prepared using poly(2-methacrylolyoxyethyl phosphorylcholine)-containing amphiphilic block copolymers. Eur Polym J. 2020;135:109885.
58. Riedel C, Gabizon R, Wilson CAM, Hamadani K, Tsekouras K, Marqusee S, et al. The heat released during catalytic turnover enhances the diffusion of an enzyme. Nature. 2015;517:227–30.
59. Kwaria RJ, Mondarte EAQ, Tahara H, Chang R, Hayashi T. Data-driven prediction of protein adsorption on self-assembled monolayers toward material screening and design. ACS Biomater Sci Eng. 2020;6:4949–56.
60. Liu Y, Zhang D, Tang Y, Zhang Y, Gong X, Xie S, et al. Machine learning-enabled repurposing and design of antifouling polymer brushes. Chem Eng J. 2021;420:129872.

Tsukuru Masuda received his Ph.D. from the University of Tokyo in 2017 under the supervision of Professor Ryo Yoshida. He was a postdoctoral researcher and a research fellow (PD) of the Japan Society for the Promotion of Science (JSPS) for Young Scientists in the group of Professor Atsushi Maruyama at the Tokyo Institute of Technology. In April 2019, he became an Assistant Professor in the group of Professor Madoka Takai at the University of Tokyo. His research interests include soft interfaces, specifically controlled radical polymerization, polymer brush surfaces, molecular interaction analysis, and machine learning modeling.